



Article

Data Compression Approach for Long-Term Monitoring of Pavement Structures

Mario Manosalvas-Paredes ^{1,*}, Nizar Lajnef ², Karim Chatti ², Kenji Aono ³, Juliette Blanc ⁴, Nick Thom ¹, Gordon Airey ¹ and Davide Lo Presti ^{1,5,*}

¹ Nottingham Transportation Engineering Centre, University of Nottingham, Nottingham NG7 2RD, UK; nicholas.thom@nottingham.ac.uk (N.T.); gordon.airey@nottingham.ac.uk (G.A.)

² Department of Civil and Environmental Engineering, Michigan State University, East Lansing, MI 48824, USA; lajnefni@egr.msu.edu (N.L.); chatti@egr.msu.edu (K.C.)

³ The Preston M. Green Department of Electrical and Systems Engineering, University of Washington St. Louis, St. Louis, MO 63130, USA; kenji@email.wustl.edu

⁴ IFSTTAR, 44340 Nantes, France; juliette.blanc@ifsttar.fr

⁵ Dipartimento di Ingegneria, Scuola Politecnica, Edificio 8, Università degli Studi di Palermo, 90128 Palermo, Italy

* Correspondence: ezzmam@nottingham.ac.uk (M.M-P.); davide.lopresti@unipa.it (D.L.P.); Tel.: +44-7848-88-5919 (M.M-P.); +44-7587-14-0422 (D.L.P.)

Received: 24 November 2019; Accepted: 20 December 2019; Published: 22 December 2019



Abstract: Pavement structures are designed to withstand continuous damage during their design life. Damage starts as soon as the pavement is open to traffic and increases with time. If maintenance activities are not considered in the initial design or considered but not applied during the service life, damage will grow to a point where rehabilitation may be the only and most expensive option left. In order to monitor the evolution of damage and its severity in pavement structures, a novel data compression approach based on cumulative measurements from a piezoelectric sensor is presented in this paper. Specifically, the piezoelectric sensor uses a thin film of polyvinylidene fluoride to sense the energy produced by the micro deformation generated due to the application of traffic loads. Epoxy solution has been used to encapsulate the membrane providing hardness and flexibility to withstand the high-loads and the high-temperatures during construction of the asphalt layer. The piezoelectric sensors have been exposed to three months of loading (approximately 1.0 million loads of 65 kN) at the French Institute of Science and Technology for Transport, Development and Networks (IFSTTAR) fatigue carousel. Notably, the sensors survived the construction and testing. Reference measurements were made with a commercial conventional strain gauge specifically designed for measurements in hot mix asphalt layers. Results from the carousel successfully demonstrate that the novel approach can be considered as a good indicator of damage progression, thus alleviating the need to measure strains in pavement for the purpose of damage tracking.

Keywords: accelerated pavement testing (APT); fatigue; piezoelectric sensor; pavement responses; longitudinal strain

1. Introduction

Flexible pavements are considered to be the most expensive assets in modern society [1]. However, pavement engineers have not found a way to delay its weakening or to provide an easy enough tool to monitor its condition during the design period [2–5]. Like any other structure, pavements age and deteriorate as a function of time which is generally accelerated by the repeated application of loads [6,7], environmental conditions [8], and by inadequate maintenance plans. Knowing the current state of a

pavement and estimating its future performance has become a matter of great importance not only for road owners but also for decision makers [9]. Following the line of structural evaluations, it is possible to separate traditional methods, developed around the use of external monitoring equipment such as the falling-weight deflectometer (FWD) [10,11], and relatively new methods, such as in-situ embedded sensors [12–16]. Early damage detection has become essential when planning future maintenance actions and budgets. Nevertheless, defining accurate damage models is usually a complicated task and sometimes impossible due to the economic cost that this could have. Mechanical responses of the damaged structure through computational simulations generally supplement this task when making comparisons between an initial state, without damage, and a final state, with damage.

Farrar and Worden [17] define damage as the change of material and/or geometric properties of the system, including changes in boundary conditions and system connectivity, a definition that has been widely accepted. They have also defined structural health monitoring (SHM) as the process in which a damage identification strategy is implemented in the infrastructure. A correct implementation of SHM must provide the necessary tools to replace traditional maintenance activities, based on time, with more practical activities which rely on the real condition of the structure. However, technical, economic, and practical challenges have been identified when implementing wired sensors. In that sense, the use of wireless sensor networks (WSNs) have increased in the past two-decades and nowadays, it is seen as a viable alternative to traditional monitoring systems [18]. Researchers at Michigan State University and Washington University at St. Louis have developed a new class of self-powered piezoelectric sensor that couples the physics of piezoelectric (energy harvesting) with the physics of low-power analog circuitry to sense, compute, and store mechanical usage statistics [19–23]. The self-powered piezoelectric sensor offers several novel features such as low power requirements (80 nW) (which is two orders of magnitude better than any commercially available technology), self-powered continuous sensing, low cost, small size, and wireless communication.

Aim of This Paper

This paper focuses on the validation of a novel data compression approach based on the statistical response of piezoelectric sensors. A successful validation will directly benefit not only pavement engineers but road agencies as a new method for monitoring real road pavement conditions will become available. These methods eliminate the need for complex models relying on the measurement of absolute strain values. The piezoelectric devices in this experiment have been exposed to three months of accelerated test, equivalent to 20 years of loading, giving robustness to the data analysis. Reference pavement measurements were collected with a conventional strain gauge. Furthermore, validating this new approach will also accelerate the usage of low-cost high-tech technology such as the piezo-floating-gate sensors [24–26].

2. Pavement Monitoring System through Piezoelectric Sensors

The data from the piezoelectric sensor is digitized using seven threshold levels while also successively storing the duration of loading events. The information is processed only when the amplitude of the input signal (voltage), coming from the thin film of polyvinylidene fluoride, exceeds one or more levels, simulating the functionality of a piezo-floating-gate system [9,21–23]. At a constant load frequency, the sensor response is visualized as a histogram of the loading distribution. Figure 1 shows a schematic representation on how the data is processed and stored.

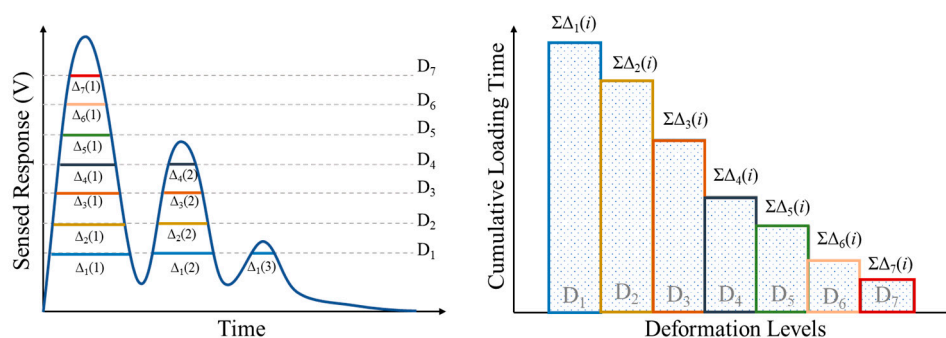


Figure 1. Representation of the data transformation and processing algorithm (redrawn from [9]).

This study assumes that the sensor results, Figure 1-right, can be characterized by the following cumulative distribution function (CDF), Equation (1), [27].

$$F(\varepsilon) = \frac{\alpha}{2} \left[1 - \operatorname{erf} \left(\frac{(\varepsilon - \mu)}{\sigma \sqrt{2}} \right) \right] \tag{1}$$

where μ is the mean of the deformation distribution, σ is the standard deviation considering load and frequency variability, and α is the total cumulative time of the applied strain. Statistical parameters μ and σ of the deformation distribution can be considered as indicators of damage progression. In fact, μ and σ are the only viable tools to analyze the results delivered by the piezoelectric sensor. These parameters are obtained by means of a curve adjustment of the sensor distribution results taken from the threshold levels (D1 to D7).

3. Accelerated Pavement Testing

The French Institute of Science and Technology for Transport, Development and Networks (IFSTTAR) under the Department of Materials and Structures is responsible for managing and handling the use of the fatigue carousel dedicated to accelerated pavement testing (APT). The carousel is composed of four arms driven by a central electrohydraulic motor that can provide different configurations of load (simple, tandem, or tridem) simulating semi-axes of heavy vehicles, see Figure 2.



Figure 2. Fatigue carousel for accelerated pavement tests, Nantes—France.

3.1. Pavement Structure and Sensor Distribution

Figure 3 shows a schematic representation of the three-layer pavement structure with embedded sensors. Figure 4 on the other hand, shows the on-site installation of the piezoelectric sensors (left-side) and commercial strain gauge (right-side) at the top of the granular material. In order to know the

on-site mechanical properties of the layers, falling-weight deflectometer (FWD) measurements were made after construction and before the start of the experiment to determine the undamaged modulus. Back-calculated results of the FWD measurements are presented in Table 1. The back-calculation process followed layer elastic theory.

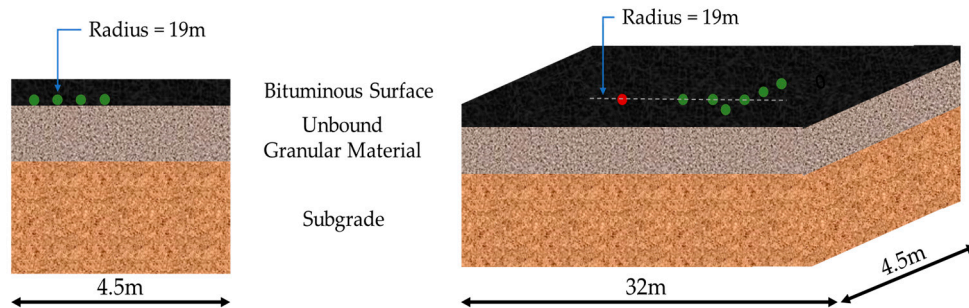


Figure 3. Schematic representation of the pavement structure with embedded sensors.



Figure 4. On-site installation of sensors in the pavement structure.

Table 1. Pavement structure back-calculation modulus.

| Layer | Thickness (mm) | Poisson's Ratio | Elastic Moduli (MPa) |
|-----------------------|----------------|-----------------|----------------------|
| Bituminous Surface | 100 | | 10,524 at 27.9 °C |
| Unbound Granular Base | 760 | 0.35 | 122 |
| Subgrade | 1600 | | 202 |

Figure 5, shows the schematic distribution of the piezoelectric sensors as well as the reference sensor along the pavement structure. As it can be seen, piezoelectric sensors are positioned 2.7 m after the reference sensor in order to reduce the effect that construction may have on the measurements. Another important point to observe is the transverse distributions of the piezoelectric sensors (H5, H6, and H8) allowing to study the effect of wandering. A brief description of the sensors is given below.

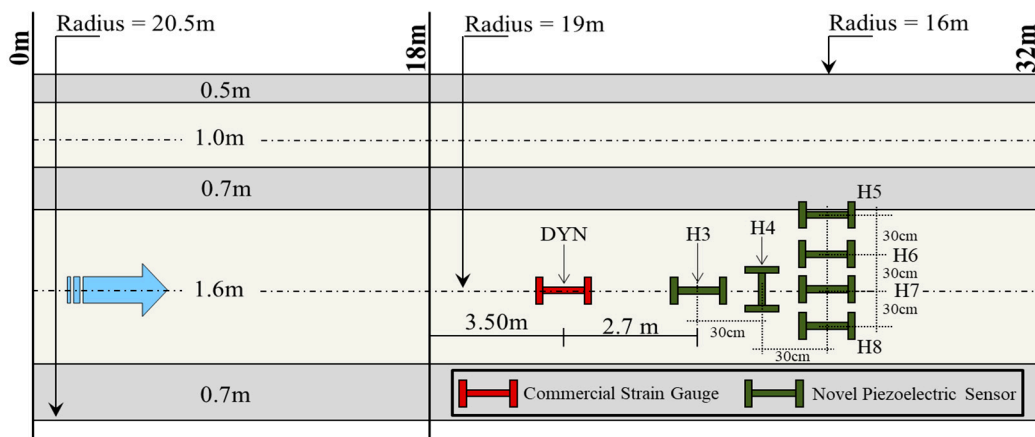


Figure 5. Schematic distribution of sensors within the pavement structure.

The used reference conventional strain gage is a precision transducer used especially for deformation measurements in hot mix asphalt. The transducer has an apparent modulus of elasticity of approximately 2.2 N/mm^2 , resistance of $120 \text{ ohms } (\Omega)$ $\frac{1}{4}$ bridge, physical range of up to $1500 \mu\epsilon$, sensitivity of $0.11 \text{ N}/\mu\epsilon$, and temperature range between -30 and $150 \text{ }^\circ\text{C}$. Equation (2) is used to transform measured voltage values (V_{out}) into deformation values where minimum voltage (V_{in}) and gauge factor (GF) have been set at 10.0 volts and 2.0 respectively.

$$\epsilon = \frac{V_{out} * GF}{V_{in}} \tag{2}$$

On the other hand, piezoelectric sensors have gained popularity in deformation and vibration measurements due to their ability to store mechanical energy from environmental variations. Under traffic loads, the piezoelectric transducer stores energy produced by the micro deformation suffered on the surface of the pavement which serves to activate the sensor. This study has used a rectangular polyvinylidene fluoride film to convert strain energy into electrical signal. Equation (3) is used to calculate the voltage (V) generated by the piezoelectric transducer where S , Y , d_{31} , h , and ϵ are the applied strain, Young’s modulus of the piezoelectric material, piezoelectric constant, thickness, and the electrical permittivity, respectively. Similarly, the generated energy (E_n) of a piezoelectric transducer through a load resistance (R) is shown in Equation (4), where t_f is the load time.

$$V = \frac{S Y d_{31} h}{\epsilon} \tag{3}$$

$$E_n = \int_0^{t_f} \frac{V^2(t)}{R} dt \tag{4}$$

3.2. Data Collection Program

Data collection started on 14 November 2017 and ended on 15 February 2018 where a total of 999,200 load applications were performed at a speed of 76.0 km/h (10.0 rotations per minute). Surface temperature varied between 0.4 and $16.8 \text{ }^\circ\text{C}$ with a mean value on surface of $9.5 \text{ }^\circ\text{C}$, and in the middle of the asphalt layer of $8.9 \text{ }^\circ\text{C}$. Sensor responses were measured at approximately every 20,000 load applications. Figure 6 shows the longitudinal deformation from the reference strain gauge and the sensor voltage after 5000 load repetitions where it can be seen how each arm of the carousel provokes a slightly difference response.

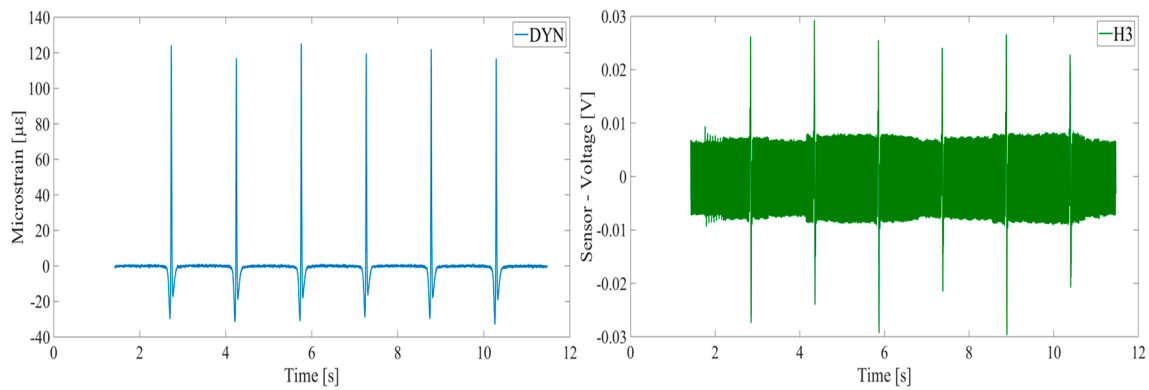


Figure 6. Measurement of strain and voltage for sensors DYN and H3 respectively.

This paper has studied the effect of wander through eleven positions, equidistant every 0.11 m. Position one is located at radius 18.48 m while position eleven is located at 19.53 m. The loading program followed a Gaussian distribution where position six, located at radius 19.0 m (see Figure 5) supports the maximum percentage of passes (22.0%), whereas positions one to five supports 1%, 3%, 7%, 11%, and 17% percentage of passes respectively.

4. Results and Discussions

This section presents the findings of the study once the APT was concluded. Figure 7 shows how the longitudinal deformation of the reference sensor, DYN, and the sensor voltage of H3 increase with the number of load repetitions. It should be noted that sensor H3 remains at the same level until 500,400 load repetitions where the main increment occurs, and changes become noticeable. Table 2 shows the maximum sensor voltages values, average of the four arms, obtained for the other piezoelectric sensors where a similar behavior is seen for the other sensors having the main increments after 500,400 loads except for sensor H8 sensor where it decreases. Sensor H8 is located at radius 19.30 m, see Figure 5.

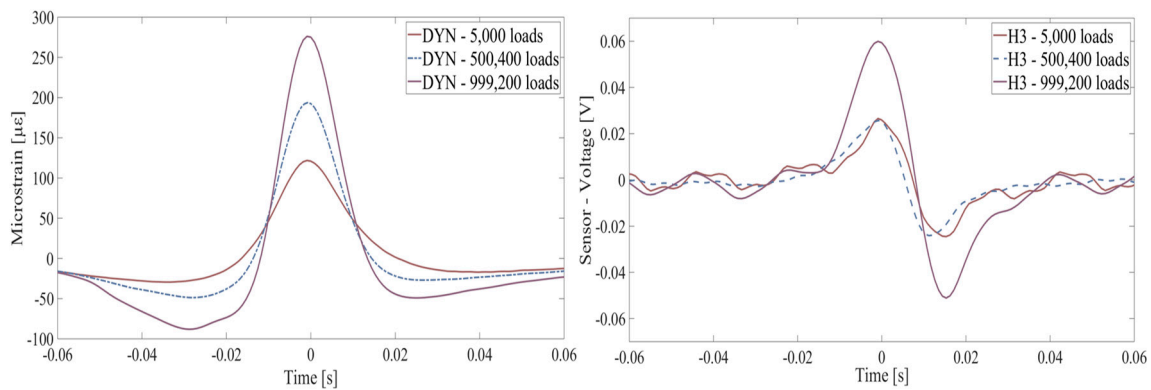


Figure 7. Measurement of strain and sensor voltage for reference and H3 sensor.

Table 2. Evolution of deformation and voltage versus number of loads.

| Number of Loads | Reference Sensor [µε] | Sensor-Voltage [V] | | | | | |
|-----------------|-----------------------|--------------------|-------|-------|-------|-------|-------|
| | | H3 | H4 | H5 | H6 | H7 | H8 |
| 5000 | 121 | 0.027 | 0.038 | 0.012 | 0.028 | 0.073 | 0.045 |
| 500,400 | 194 | 0.026 | 0.017 | 0.011 | 0.012 | 0.055 | 0.044 |
| 999,200 | 276 | 0.059 | 0.041 | 0.014 | 0.027 | 0.067 | 0.010 |

Figure 8 on the other hand shows the evolution of the longitudinal microstrain (DYN) and sensor voltage (H3) during the 999,200 load repetitions. It is necessary to highlight how both trends

correspond to each other especially at 136,800 and 507,000 load repetitions where the signal decrease and increase respectively. The responses decrease at 136,800 load repetitions as the pavement starts to heal itself as the result of letting it rest without applying load on the surface. However, this “healing” process is rapidly lost once the loading program restarts. On the other hand, at around 507,000 load repetitions both responses show a change in their slopes indicating that damage has increased and is now spreading its way to the surface.

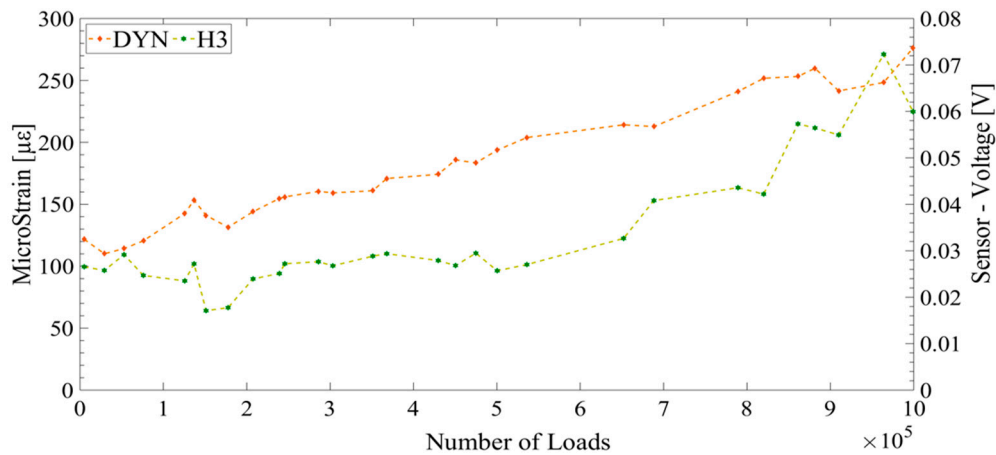


Figure 8. Comparison of strain (DYN) and sensor voltage (H3) at radius 19.0 m.

Figures 9 and 10 show the effect that varying the load “wandering” has on the measured responses. From these figures, it can be seen how both responses decrease their values as the load moves away from the center (position six, radius 19.0 m). This is seen for the reference sensor (DYN) as well as for piezoelectric sensors (H3, H4, and H7) also located at radius 19.0 m, see Figure 5. On the other hand, sensor H5 located at radius 18.40 m which receives merely 1% of the total load passes, is the one showing the lower values since most of the time the load is far away from the location of the sensor. Finally, sensors H6 and H8 show how the measured responses fades with respect to the load positioning.

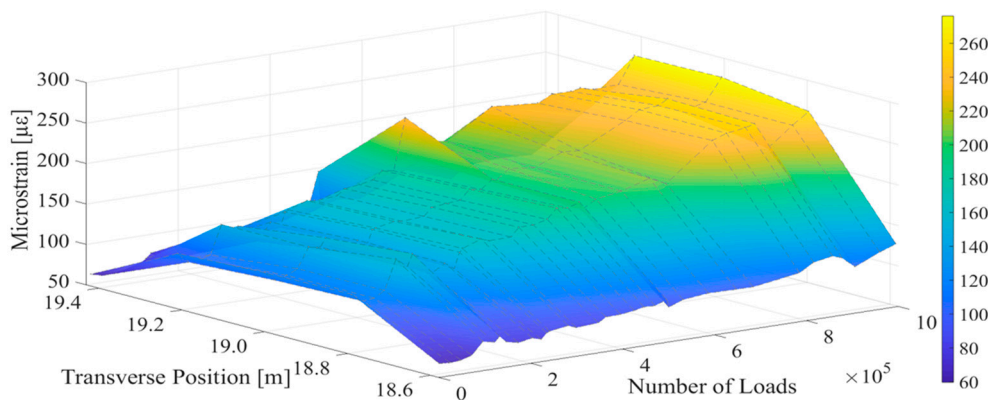


Figure 9. Evolution of deformation versus number of loads and transversal position.

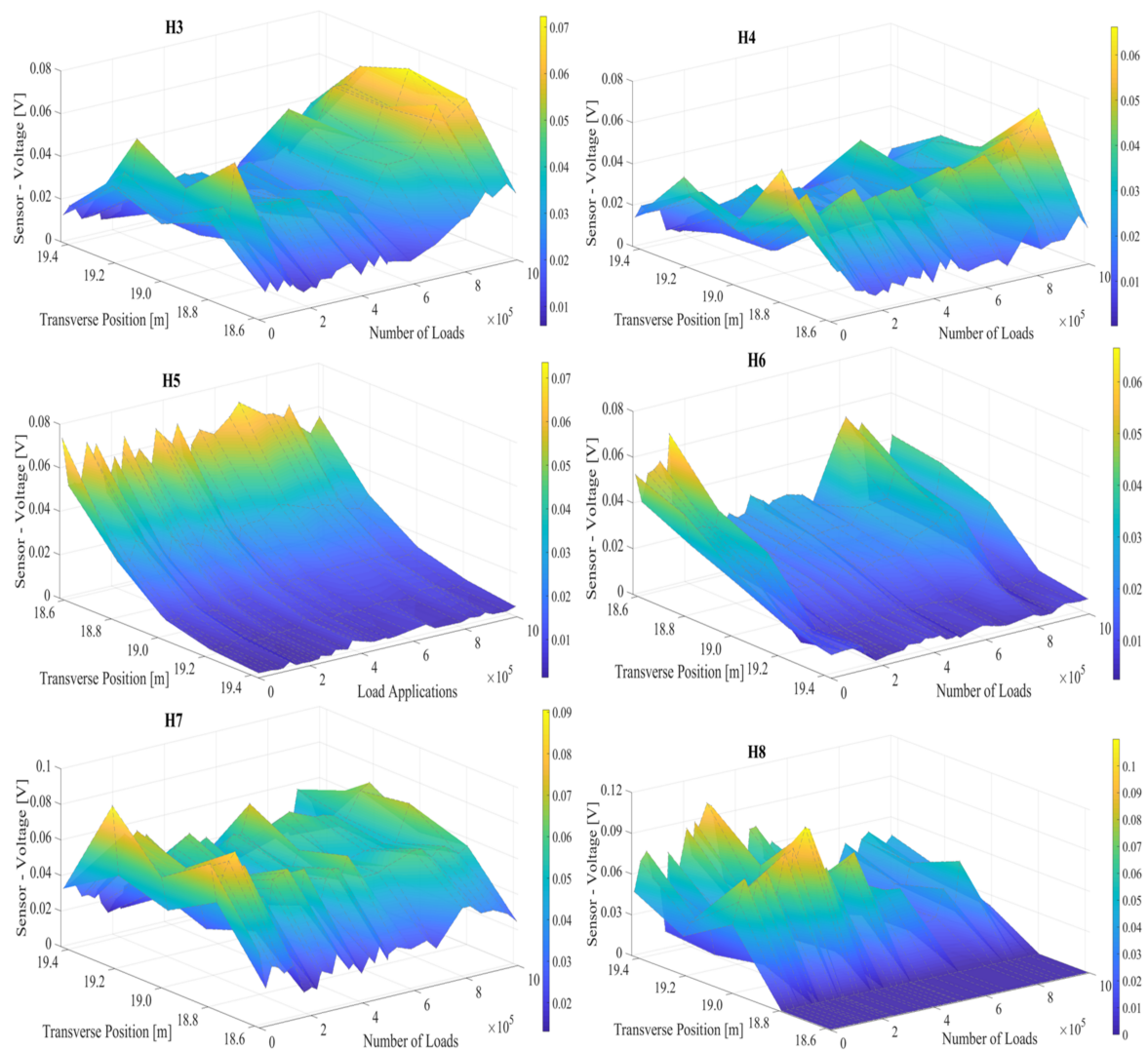


Figure 10. Sensor-voltage evolution versus number of loads and transverse position.

A correct definition of the threshold levels, Figure 1-left, is essential for the proposed approach. This paper has used percentiles P-95 and P-05 to define the upper and lower limits based on the entire signal. Figure 8 shows the evolution of sensor H3 during the 999,200 load repetitions where the maximum average response (0.0723 V) is seen at 964,000 load repetitions whereas the minimum average response (0.0171 V) is seen at 151,200 load repetitions. Following percentiles P-95 and P-05, the upper and lower limits are calculated and shown in Table 3.

Table 3. Definition of threshold levels for novel data compression approach.

| Level Number | H3 | H4 | H7 |
|--------------|-------|-------|-------|
| D1 | 0.018 | 0.028 | 0.041 |
| D2 | 0.025 | 0.033 | 0.048 |
| D3 | 0.031 | 0.039 | 0.054 |
| D4 | 0.038 | 0.044 | 0.061 |
| D5 | 0.045 | 0.049 | 0.067 |
| D6 | 0.051 | 0.055 | 0.074 |
| D7 | 0.058 | 0.060 | 0.080 |

Once the seven thresholds have been defined, the measured average signals are then subdivided in order to measure the time that each level is open. Figures 11–13 show the novel data compression approach for sensors H3, H4, and H7 respectively.

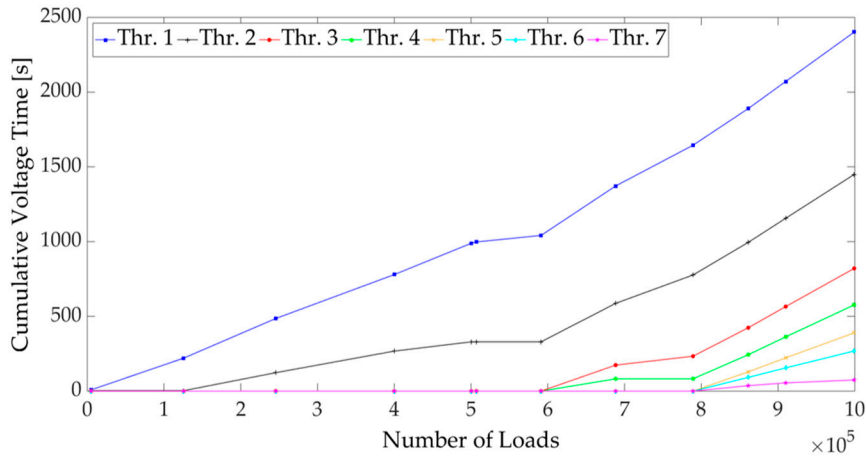


Figure 11. Cumulative voltage time for H3.

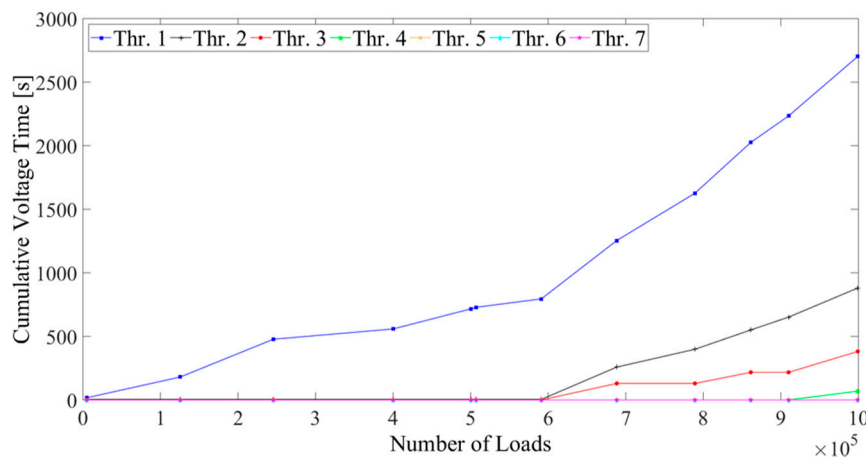


Figure 12. Cumulative voltage time for H4.

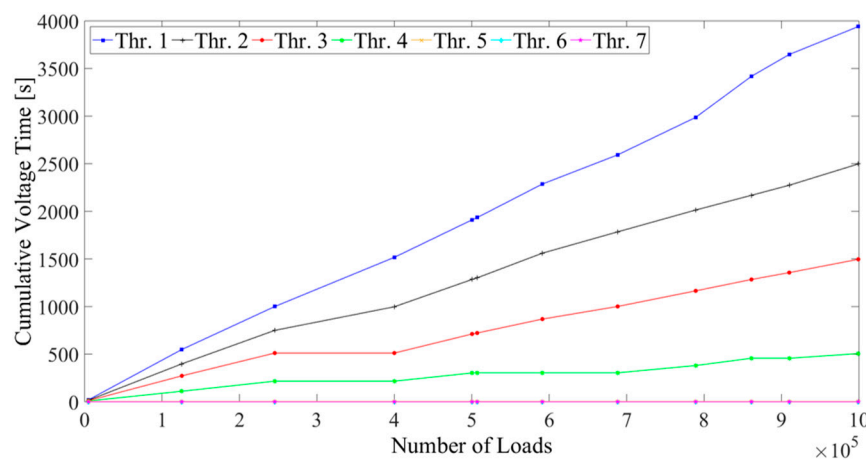


Figure 13. Cumulative voltage time for H7.

Finally, Table 4 show the activation times in terms of number of repetitions for the upper threshold levels. Activation “wake-up” time means that the measured average signal (voltage) has exceeded the threshold levels at a certain number of loads. Level wake-up times are directly related to the appearance of damage in terms of surface cracking on the pavement structure.

Table 4. Threshold activation versus number of loads.

| Level Number | H3 | H4 | H7 |
|--------------|---------|---------|---------|
| D3 | 591,200 | 591,200 | 125,600 |
| D4 | 591,200 | 910,000 | 125,600 |
| D5 | 789,200 | N/A | N/A |
| D6 | 789,200 | N/A | N/A |
| D7 | 789,200 | N/A | N/A |

As shown above, sensor H3 is the one providing the best results for assessing damage in the structure. In essence, when the amplitude of the strain increases under the influence of repetitive loads, the stored voltage also increases, resulting in the activation of higher thresholds. Figure 14 shows the condition of the pavement structure at the end of the experiment. Two paint colors, white and blue, were used to illustrate the appearance of cracks with time. Paint color white denotes surface cracking after 1.0 million load repetitions, whereas color blue denotes later cracking.



Figure 14. Surface condition of the pavement at the end of the experiment.

5. Conclusions

This study has successfully validated, through full-scale testing, the usefulness of embedding piezoelectric sensors in pavement structures for long-term monitoring. The innovation of the proposed data compression approach relies in using cumulative pavement responses instead of single measurements (i.e., longitudinal strains) which are highly dependent on external conditions.

This study has found that the cumulative loading time of piezo voltage can be considered as a good indicator of damage progression while different activation times for the threshold levels can also be considered as good indicator of damage severity.

From the results presented above, this study can conclude that the observations made using the reduced data obtained from the piezoelectric sensors, which are significantly cheaper and easier to install, match the observations obtained using reference strain gages that continuously measure the

strain response, which is impractical for long term monitoring. Both technologies provide similar trends in terms of damage growth.

Finally, the next steps will focus on scaling up the implementation and testing of the piezoelectric sensors and associated data management approaches.

Author Contributions: Conceptualization, M.M.-P. and N.L.; testing, M.M.-P., J.B., and K.A.; software, M.M.-P., N.L., and K.C.; validation, M.M.-P., K.C., K.A., and N.L.; formal analysis, M.M.-P., K.C., and N.L.; investigation, M.M.-P., K.C., and N.L.; resources, M.M.-P., N.T., G.A., D.L.P., and N.L.; data curation, M.M.-P., K.C., and N.L.; writing—original draft preparation, M.M.-P.; writing—review and editing, M.M.-P., K.A., N.T., G.A., K.C., and N.L.; visualization, M.M.-P. and N.L. All authors have read and agreed to the published version of the manuscript.

Funding: This work was supported in part by the National Science Foundation (award CNS 1645783). This work was carried out within the H2020 SMARTI ETN programme receiving funding from the European Union’s H2020 Programme for research, technological development and demonstration under grant agreement number 721493. Finally, this work was supported in part the Italian Ministry of University and Research (MIUR dm n.372 08/05/18).

Acknowledgments: The Accelerated Pavement Testing was carried out within the BioRePavation project. It was co-funded by Funding Partners of The ERA-NET plus Infravation and the European Union’s Seventh Framework Programme for research, technological development, and demonstration under grant agreement number 607524.

Conflicts of Interest: N.L. is the co-founder of Piezonix LLC, a startup commercializing the self-powered floating gate sensing technology. The other authors declare no conflict of interest. The funders had no role in the design of the study; in the collection, analyses, or interpretation of data; in the writing of the manuscript, or in the decision to publish the results.

References

1. National Asphalt Pavement Association; European Asphalt Pavement Association. *The Asphalt Paving Industry A Global Perspective*, 3rd ed.; National Asphalt Pavement Association: Brussels, Belgium; European Asphalt Pavement Association: Brussels, Belgium, 2011; ISBN 0-914313-06-1.
2. Xue, W.; Wang, D.; Wang, L. A review and perspective about pavement monitoring. *Int. J. Pavement Res. Technol.* **2012**, *5*, 295–302.
3. Brown, S.F. Developments in pavement structural design and maintenance. *Proc. Instn. Civ. Engrs. Transp.* **1998**, *129*, 201–206.
4. Robbins, M.M.; Rodezno, C.; Tran, N.; Timm, D.H. Pavement ME Design—A Summary of Local Calibration Efforts for Flexible Pavements. *NCAT Rep.* **2017**, 1–98.
5. Ullidtz, P.; Ertman Larsen, H.J. State-of-the-Art Stress, Strain and Deflection Measurements. In *Symposium on the State-of-the-Art of Pavement Response Monitoring Systems for Roads and Airfields*; US Army Corps of Engineers: Washington, DC, USA, 1989; pp. 148–161.
6. Dessouky, S.H.; Al-Qadi, I.L.; Yoo, P.J. Full-depth flexible pavement responses to different truck tyre geometry configurations. *Int. J. Pavement Eng.* **2014**, *15*, 512–520. [[CrossRef](#)]
7. Brown, S.F.; Peattie, K.R. The structural design of bituminous pavements for heavy traffic. *Third Int. Conf. Struct. Des. Asph. Pavements* **1974**, *57*, 83–97.
8. Leiva-Villacorta, F.; Vargas-Nordbeck, A.; Aguiar-Moya, J.P.; Loria-Salazar, L. Development and calibration of permanent deformation models. In *Roles of Accelerated Pavement Testing in Pavement Sustainability*; Springer International Publishing: Cham, Switzerland, 2016; pp. 573–587.
9. Lajnef, N.; Chatti, K.; Chakrabartty, S.; Rhimi, M.; Sarkar, P. *Smart Pavement Monitoring System*; Federal Highway Administration: Washington, DC, USA, 2013.
10. Verma, S.K.; Bhadauria, S.S.; Akhtar, S.; Verma, S.K.; Bhadauria, S.S.; Akhtar, S. Review of Nondestructive Testing Methods for Condition Monitoring of Concrete Structures. *J. Constr. Eng.* **2013**, *2013*, 1–11. [[CrossRef](#)]
11. Marecos, V.; Fontul, S.; de Lurdes Antunes, M.; Solla, M. Evaluation of a highway pavement using Non-Destructive Tests: Falling Weight Deflectometer and Ground Penetrating Radar. *Constr. Build. Mater.* **2017**, *154*, 1164–1172. [[CrossRef](#)]
12. Xue, W.; Wang, L.; Wang, D.; Druta, C. Pavement Health Monitoring System Based on an Embedded Sensing Network. *J. Mater. Civ. Eng.* **2014**, *26*, 04014072. [[CrossRef](#)]
13. Lajnef, N.; Rhimi, M.; Chatti, K.; Mhamdi, L.; Faridazar, F. Toward an Integrated Smart Sensing System and Data Interpretation Techniques for Pavement Fatigue Monitoring. *Comput. Civ. Infrastruct. Eng.* **2011**, *26*, 513–523. [[CrossRef](#)]

14. Sohn, H.; Ferrar, C.; Hemez, F.M.; Czarnecki, J. *A Review of Structural Health Monitoring Literature: 1996–2001*; Los Alamos National Laboratory: Los Alamos, NM, USA, 2003.
15. Duong, N.S.; Blanc, J.; Hornych, P.; Bouveret, B.; Carroget, J.; Le feuvre, Y. Continuous strain monitoring of an instrumented pavement section. *Int. J. Pavement Eng.* **2018**, *8436*, 1–16. [[CrossRef](#)]
16. Duong, N.S.; Blanc, J.; Hornych, P.; Menant, F.; Lefeuvre, Y.; Bouveret, B. Monitoring of pavement deflections using geophones. *Int. J. Pavement Eng.* **2018**. [[CrossRef](#)]
17. Farrar, C.R.; Worden, K. An introduction to structural health monitoring. *Philos. Trans. R. Soc. A Math. Phys. Eng. Sci.* **2007**, *365*, 303–315. [[CrossRef](#)] [[PubMed](#)]
18. Lynch, J.; Loh, K. A Summary Review of Wireless Sensors and Sensor Networks for Structural Health Monitoring. *Shock Vib. Dig.* **2006**, *38*, 91–128. [[CrossRef](#)]
19. Huang, C.; Lajnef, N.; Chakrabartty, S. Calibration and characterization of self-powered floating-gate usage monitor with single electron per second operational limit. *IEEE Trans. Circuits Syst. I Regul. Pap.* **2010**, *57*, 556–568. [[CrossRef](#)]
20. Rhimi, M.; Lajnef, N.; Chatti, K.; Faridazar, F. A self-powered sensing system for continuous fatigue monitoring of in-service pavements. *Int. J. Pavement Res. Technol.* **2012**, *5*, 303–310.
21. Chakrabartty, S.; Lajnef, N.; Elvin, N.; Gore, A. Self-Powered Sensor. U.S. Patent 8,056,420, 2008.
22. Hasni, H.; Alavi, A.H.; Jiao, P.; Lajnef, N.; Chatti, K.; Aono, K. A new approach for damage detection in asphalt concrete pavements using battery-free wireless sensors with non-constant injection rates. *Measurement* **2017**, *110*, 217–229. [[CrossRef](#)]
23. Hasni, H.; Alavi, A.H.; Chatti, K.; Lajnef, N. A self-powered surface sensing approach for detection of bottom-up cracking in asphalt concrete pavements: Theoretical/numerical modeling. *Constr. Build. Mater.* **2017**, *144*, 728–746. [[CrossRef](#)]
24. Aono, K.; Hasni, H.; Pochettino, O.; Lajnef, N. Quasi-Self-Powered Piezo-Floating-Gate Sensing Technology for Continuous Monitoring of Large-Scale Bridges. *Frontiers Built Environ.* **2019**, *5*, 29. [[CrossRef](#)]
25. Aono, K. Self-powered Sensors to Facilitate Infrastructural Internet-of-Things for Smart Structures Self-powered Sensors to Facilitate Infrastructural Internet-of-Things for Smart Structures. In Proceedings of the 13th International Workshop on Advanced Smart Materials and Smart Structures Technology, Tokyo, Japan, 22–23 July 2017.
26. Aono, K.; Covassin, T.; Chakrabartty, S. *Monitoring of Repeated Head Impacts Using Time-Dilation Based Self-Powered Sensing*; IEEE: Melbourne, Australia, 2014; pp. 1620–1623.
27. Alavi, A.H.; Hasni, H.; Lajnef, N.; Chatti, K.; Faridazar, F. An intelligent structural damage detection approach based on self-powered wireless sensor data. *Autom. Constr.* **2016**, *62*, 24–44. [[CrossRef](#)]



© 2019 by the authors. Licensee MDPI, Basel, Switzerland. This article is an open access article distributed under the terms and conditions of the Creative Commons Attribution (CC BY) license (<http://creativecommons.org/licenses/by/4.0/>).